A SEPARABLE STRONG-ANISOTROPY APPROXIMATION FOR PURE QP WAVE PROPAGATION IN TRANSVERSELY ISOTROPIC MEDIA

J. Schleicher and J. C. Costa

email: *js@ime.unicamp.br*

keywords: *Pseudo-S wave, VTI media, wave propagation, dispersion relation, low rank, separable approximation*

ABSTRACT

The qP and qS-wave eikonal equations derived from the VTI wave equation show that in the pseudo-acoustic approximation, their dispersion relations degenerate into a single one. Therefore, when using this dispersion relation for wave simulation, for instance by means of finite-difference approximations, both events are generated. To avoid the occurrence of the pseudo-S wave, the qP-wave dispersion relation alone needs to be approximated. This can be done with or without the pseudo-acoustic approximation. A Padé approximation of the square root led to the best approximation. An implementation of a low-rank approximation to this equation demonstrates that this can provide high-accuracy wavefields even in strongly anisotropic inhomogeneous media. It can be further approximated in a separable way for an efficient implementation in the time-wavenumber domain. Our numerical experiments demonstrate that this separable approximation remains valid up to very strong anisotropy.

INTRODUCTION

The pseudo-acoustic approximation (Alkhalifah, 1998, 2000) is a very cost-effective approach to anisotropic RTM. The pseudo-acoustic wave equation, proposed to model the evolution of qP modes, is derived under the assumption that shear velocity is zero along the symmetry axis.

However, finite difference implementations of pseudo-acoustic wave equation can be plagued by physical instability and undesirable S-wave modes even in the weakly anisotropic regime. Several strategies have been proposed to overcome these problems. Stability of space-time FD implementations of the pseudo-acoustic wave equation can be only be assured if the Thomsen parameters satisfy the constraint $\epsilon \geq \delta$, which is not always valid for shales (Thomsen, 1986). Fletcher et al. (2009) and Fowler et al. (2010) showed that a stable approximation for qP modes in VTI media can be derived if one does not assume the shear velocity along the symmetry axis to be zero. However, their proposed stable coupled system of second-order differential equations still can produce undesirable S-wave modes.

The mitigation of the S-wave in FD implementations of the pseudo-acoustic approximation has been an area of active research since the original work of Alkhalifah (1998). For example, Alkhalifah (2003) indicated that if the source is in an isotropic region the S modes are not generated, although it still can be produced at interfaces with sharp contrast. The work of Grechka et al. (2004) indicates that the instability of pseudo-acoustic wave-equation is due to the coupling of the S mode to the qP mode. The S mode is not stable when $\epsilon \geq \delta$. Other removal strategies include the choice of a finite shear-wave velocity (Fletcher et al., 2009) to achieve a zero shear-wave reflection coefficient everywhere in the model. However, this introduces an additional parameter and is hard to generalize to orthorhombic media. The propagation filter of Le and Levin (2014) is cumbersome, because it requires eigenvalue decomposition.

For this reason, a very successful solution to obtain a stable qP wave equation is to factor out these spurious modes from the pseudo-acoustic wave equation. The work of Klíe and Toro (2001) presents one such approximation for pure qP wave-equation under the assumption of weak anisotropy. Exact factorization results in a pseudo-differential operator in the mixed space-wavenumber domain (Liu et al., 2009). Differential equations in space-time for the pure qP mode can be derived through approximations to the exact pseudo-differential operator for qP evolution. Liu et al. (2009) proposed an algorithm to implement the exact factorization of the pseudo-acoustic wave equation in the mixed space-wavenumber domain. Pestana et al. (2012) derive an alternative approximation for the exact factorization which is valid for weak anisotropy and can be implemented using finite difference in time and pseudo-spectral method in space. Zhan et al. (2013) show how to generalize this implementation to TTI media. More sophisticated approximations of this factorization can be found in Du et al. (2014). Most recently, the exact factorization of the pseudo-acoustic wave equation in the mixed space-wavenumber domain has been implemented using the low-rank approximation (Fomel et al., 2013; Song and Alkhalifah, 2013; Wu and Alkhalifah, 2014; Sun et al., 2016).

In last year's report, Schleicher and Costa (2014) derived a new pure qP-mode approximation free of physical instability and S modes and valid even for strongly anisotropic media. Based on this new equation, we derive in this year's report a separable approximation that allows for pseudo-spectral implementation in the mixed space-wavenumber domain. This allows to explore its potential to provide an approximation that factors heterogeneity and anisotropy even in strongly anisotropic media in the fashion used by Liu et al. (2009) and Pestana et al. (2012) for weak anisotropy. We also compare the resulting wave-propagation simulations in smoothly heterogeneous media and in a more realistic model to corresponding solutions obtained with a low-rank approximation of the original dispersion relation.

THEORY

Elastic wave propagation in a VTI medium

For completeness, we start with a short summary of the approximate dispersion relation for qP waves. For details, please refer to last year's report (Schleicher and Costa, 2014). The derivation starts at the approximate elastic wave equation for VTI media with small δ, as specified by Bloot et al. (2013). Substitution of a zero-order ray ansatz (Červený, 1985; Červený, V., 2001) into the VTI wave equation without a source term yields the familiar ray-tracing eigenvalue problem, where the eigenvalues must all be equal to one. Bloot et al. (2013) expressed the Christoffel matrix can be expressed explicitely to find the qP and qS eigenvalues as

$$\Lambda_{1,2} = \frac{1}{2}\left((\alpha^2+\beta^2)\|\mathbf{p}\|^2 + 2\epsilon\alpha^2\|\widehat{\mathbf{p}}\|^2 \pm \sqrt{(\alpha^2-\beta^2)^2\|\mathbf{p}\|^4 + 4\Pi}\right) \tag{1}$$

where the slowness vector $\mathbf{p}$ is defined as

$$\mathbf{p} = \nabla T = (p_1, p_2, p_3)\ . \tag{2}$$

Moreover,

$$\alpha = \sqrt{\frac{\lambda+2\mu}{\rho}} \qquad \text{and} \qquad \beta = \sqrt{\frac{\mu}{\rho}} \tag{3}$$

denote the vertical P and S wave velocities, and ϵ and δ are the Thomsen parameters. Also, the horizontal slowness vector $\widehat{\mathbf{p}}$ is given by

$$\widehat{\mathbf{p}} = \widehat{\nabla} T = (p_1, p_2, 0)\ , \tag{4}$$

and, up to first order in δ,

$$\Pi \approx \alpha^2\left[(\alpha^2-\beta^2)\left(\epsilon\|\mathbf{p}\|^2 + 2(\delta-\epsilon)p_3^2\right) + \alpha^2\epsilon^2\|\widehat{\mathbf{p}}\|^2\right]\|\widehat{\mathbf{p}}\|^2. \tag{5}$$

The condition that the eigenvalues must be equal to one in order to correspond to a solution to the eigenvalue problem translates thus into

$$\Lambda_{1,2} = A_+ \pm \sqrt{A_-^2 - B} = 1 \tag{6}$$

where

$$A_{\pm} = \frac{1}{2}\left((\alpha^2 \pm \beta^2)\|\mathbf{p}\|^2 + 2\epsilon\alpha^2\|\widehat{\mathbf{p}}\|^2\right) \quad (7)$$

$$B = 2\alpha^2(\alpha^2 - \beta^2)(\epsilon - \delta)p_3^2\|\widehat{\mathbf{p}}\|^2 \,. \quad (8)$$

Equation (6) with a positive sign is the qP eikonal equation that describes the kinematic properties of qP-wave propagation, and with a negative sign it is the qSV eikonal equation.

Pseudo-acoustic approximation

The pseudo-acoustic approximation (Alkhalifah, 1998, 2000) consists of setting the vertical S-wave velocity to zero in the equations governing wave propagation. With $\beta = 0$, equation (6) becomes (Schleicher and Costa, 2014)

$$\Lambda_{1,2} = a \pm \sqrt{a^2 - b} = 1 \,, \quad (9)$$

where now

$$a = \frac{\alpha^2}{2}\left(\|\mathbf{p}\|^2 + 2\epsilon\|\widehat{\mathbf{p}}\|^2\right) \,, \quad (10)$$

$$b = 2\alpha^4(\epsilon - \delta)p_3^2\|\widehat{\mathbf{p}}\|^2 \,. \quad (11)$$

A simple analysis of equation (9) reveals that it can be rewritten as

$$\begin{aligned} \pm\sqrt{a^2 - b} &= 1 - a \\ a^2 - b &= 1 - 2a + a^2 \\ \text{or} \quad 2a - b &= 1 \,, \end{aligned} \quad (12)$$

i.e.,

$$\alpha^2\left(\|\mathbf{p}\|^2 + 2\epsilon\|\widehat{\mathbf{p}}\|^2\right) - 2\alpha^4(\epsilon - \delta)p_3^2\|\widehat{\mathbf{p}}\|^2 = 1 \,. \quad (13)$$

Replacing $\|\widehat{\mathbf{p}}\|^2 \to \frac{k_r^2}{\omega^2}$, $p_3^2 \to \frac{k_z^2}{\omega^2}$, $\alpha^2 \to \frac{v_n^2}{1+2\delta}$, $\frac{\epsilon - \delta}{1+2\delta} \to \eta$, where k_r and k_z denote the horizontal and vertical wavenumbers and v_n is the NMO velocity, we arrive at

$$k_z^2 = \frac{v_n^2}{\alpha^2}\left(\frac{\omega^2}{v_n^2} - \frac{\omega^2\, k_r^2}{\omega^2 - 2\eta v_n^2\, k_r^2}\right) \,, \quad (14)$$

which is exactly the pseudo-acoustic qP dispersion relation of Alkhalifah (2000). Since in the analysis leading to equation (12), we have taken into account both signs in front of the square root, this equation is actually a dispersion relation for both, qP and qSV waves.

For this reason, Schleicher and Costa (2014) concluded that a description of pure qP wave propagation must directly use equation (9) with a positive sign. Better still, since equation (6) has the same structure, any approximation that is made to equation (9) to allow for efficient implementation can be made in the same way to the full equation (6) with no need for the pseudo-acoustic approximation.

Non-acoustic qP eikonal equation

For $B \ll A_-^2$, we find the approximate square root (Schleicher and Costa, 2014)

$$\sqrt{A_-^2 - B} \approx A_- - \frac{B}{2A_-} \,, \quad (15)$$

which leads to the approximate eikonal equation

$$A_+ + A_- - \frac{B}{2A_-} \approx 1 \,, \quad (16)$$

or, with $A_+ + A_- = 2a$ (compare equations (7) and (10)),

$$2A_-(2a-1) = B\,. \tag{17}$$

i.e.,

$$\left((\alpha^2-\beta^2)\|\mathbf{p}\|^2 + 2\epsilon\alpha^2\|\widehat{\mathbf{p}}\|^2\right)\left(\alpha^2(\|\mathbf{p}\|^2 + 2\epsilon\|\widehat{\mathbf{p}}\|^2) - 1\right) = 2\alpha^2(\alpha^2-\beta^2)(\epsilon-\delta)p_3^2\|\widehat{\mathbf{p}}\|^2\,. \tag{18}$$

The corresponding dispersion relation reads

$$\left([(1+2\eta)v_n^2 - \beta^2]k_r^2 + (\alpha^2-\beta^2)k_z^2\right)\left((1+2\eta)v_n^2k_r^2 + \alpha^2k_z^2 - \omega^2\right) = 2\eta v_n^2(\alpha^2-\beta^2)k_r^2k_z^2\,. \tag{19}$$

This equation has been derived in a different way by Pestana et al. (2012), based on a factorization of the dispersion relation by Du et al. (2008).

Equation (17) allows for propagation even for $\eta < 0$. It shows only a weak dependence on β and reduces to the equation of Klíe and Toro (2001) for $\beta = 0$. This means that this dispersion relation might be used to improve on Klíe and Toro's equation by using a constant ratio between the vertical P and S-wave velocities, in this way still using the same number of parameters required in that equation.

Strong-anisotropy approximation For values of B close to A_-^2, this approximation may not have sufficient quality. Schleicher and Costa (2014) achieved a better approximation of the square root by means of a fractional Padé approximation, i.e.,

$$A_-\sqrt{1-\frac{B}{A_-^2}} \approx A_-\left(1 - \frac{q_1\frac{B}{A_-^2}}{1-q_2\frac{B}{A_-^2}}\right)\,, \tag{20}$$

where q_1 and q_2 are the Padé coefficients. The corresponding approximate eikonal equation reads

$$A_+ + A_- - \frac{q_1\frac{B}{A_-}}{1-q_2\frac{B}{A_-^2}} \approx 1 \tag{21}$$

or, equivalently,

$$(A_-^2 - q_2B)(2a-1) = q_1A_-B\,. \tag{22}$$

Explicitly, it becomes

$$\begin{aligned}\left[\left((\alpha^2-\beta^2)\|\mathbf{p}\|^2 + 2\epsilon\alpha^2\|\widehat{\mathbf{p}}\|^2\right)^2 - 8q_2\alpha^2(\alpha^2-\beta^2)(\epsilon-\delta)p_3^2\|\widehat{\mathbf{p}}\|^2\right]\left(\alpha^2(\|\mathbf{p}\|^2 + 2\epsilon\|\widehat{\mathbf{p}}\|^2) - 1\right)\\ = 4q_1\left((\alpha^2-\beta^2)\|\mathbf{p}\|^2 + 2\epsilon\alpha^2\|\widehat{\mathbf{p}}\|^2\right)\alpha^2(\alpha^2-\beta^2)(\epsilon-\delta)p_3^2\|\widehat{\mathbf{p}}\|^2\,,\end{aligned} \tag{23}$$

which yields the dispersion relation

$$\begin{aligned}\left[\left([(1+2\eta)v_n^2 - \beta^2]k_r^2 + (\alpha^2-\beta^2)k_z^2\right)^2 - 8q_2\eta v_n^2(\alpha^2-\beta^2)k_r^2k_z^2\right]\left((1+2\eta)v_n^2k_r^2 + \alpha^2k_z^2 - \omega^2\right)\\ = 4q_1\left([(1+2\eta)v_n^2 - \beta^2]k_r^2 + (\alpha^2-\beta^2)k_z^2\right)\eta v_n^2(\alpha^2-\beta^2)k_r^2k_z^2\,.\end{aligned} \tag{24}$$

Schleicher and Costa (2014) showed that this approximation is highly accurate even for strong anisotropy when choosing anisotropy-dependent values for the Padé coefficients q_1 and q_2.

Separable approximations

The problem with the above approximations is that they are unsuitable for efficient wave-propagation simulation in the time-wavenumber domain in heterogeneous media. The most feasible way to solve them is using low-rank approximations, which can be very demanding on storage and computational cost for strongly heterogeneous media. In this sense, they provide no advantage over the full qP eikonal equation (6) involving a square root, which can also be solved using a low-rank approximation. For an efficient implementation in the spectral domain, a separable approximation is required. The computational cost of separable approximations does not depend on the medium heterogeneity.

Linear approximation For this reason, Pestana et al. (2012) introduce an additional approximation to their version of the dispersion relation. They express their approximation of the dispersion relation (here obtained from the linear approximation of the square root) as

$$\omega^2 = (1+2\eta)v_n^2 k_r^2 + \alpha^2 k_z^2 - \frac{2\eta v_n^2 k_r^2 k_z^2}{k_z^2 + F k_r^2} \,, \tag{25}$$

where they use the notations

$$F = \frac{(1+2\eta)v_n^2 - \beta^2}{\alpha^2 - \beta^2} = 1 + \frac{2\epsilon}{f}, \quad \text{and} \quad f = 1 - \frac{\beta^2}{\alpha^2} \,. \tag{26}$$

The separable approximation proposed by the cited authors is to use $F \approx 1$, which eliminates the S-wave velocity from the approximation. Note however, that this is a stronger assumption than the pseudo-acoustic approximation which sets $\beta = 0$.

Second-order approximation The corresponding version of the strong-anisotropy approximation (24) reads

$$\omega^2 = (1+2\eta)v_n^2 k_r^2 + \alpha^2 k_z^2 - 2q_1 \frac{2\eta v_n^2 k_r^2 k_z^2}{k_z^2 + F k_r^2 - 4q_2 G} \,, \tag{27}$$

where

$$G = \frac{2(\epsilon - \delta)}{f} \frac{k_r^2 k_z^2}{k_z^2 + F k_r^2} \,. \tag{28}$$

For $q_1 = 1/2$ and $q_2 = 0$, it reduces to equation (25).

To obtain a separable approximation that remains valid for strong anisotropy, we first put $k^2 = k_r^2 + k_z^2$ into evidence in the denominator of equation (27) and then approximate the resulting expression up to first order in the anisotropy parameters. In symbols,

$$\begin{aligned} \omega^2 &= (1+2\eta)v_n^2 k_r^2 + \alpha^2 k_z^2 - 2q_1 \frac{2\eta v_n^2 k_r^2 k_z^2}{k^2 \left(1 + \frac{2\epsilon}{f}\frac{k_r^2}{k^2} - \frac{4q_2 G}{k^2}\right)} \\ &\approx (1+2\eta)v_n^2 k_r^2 + \alpha^2 k_z^2 - 2q_1 \frac{2\eta v_n^2 k_r^2 k_z^2}{k^2} \left(1 - \frac{2\epsilon}{f}\frac{k_r^2}{k^2} - \frac{4q_2 G}{k^2}\right) \,. \end{aligned} \tag{29}$$

Next, we approximate G correspondingly, i.e.,

$$\begin{aligned} G &= \frac{2(\epsilon - \delta)}{f} \frac{k_r^2 k_z^2}{k^2 \left(1 + \frac{2\epsilon}{f}\frac{k_r^2}{k^2}\right)} \\ &\approx \frac{2(\epsilon - \delta)}{f} \frac{k_r^2 k_z^2}{k^2} \left(1 - \frac{2\epsilon}{f}\frac{k_r^2}{k^2}\right) \,. \end{aligned} \tag{30}$$

Substitution of equation (30) in equation (29) yields, up to third order in $1/k^2$,

$$\omega^2 \approx (1+2\eta)v_n^2 k_r^2 + \alpha^2 k_z^2 - 2q_1 \frac{2\eta v_n^2 k_r^2 k_z^2}{k^2} \left(1 - \frac{2\epsilon}{f}\frac{k_r^2}{k^2} - \frac{8q_2(\epsilon - \delta)}{f}\frac{k_r^2 k_z^2}{k^4}\right) \,. \tag{31}$$

Alternatively, we can use $f = 1 - \beta^2/\alpha^2$ and assume that the velocity ratio is also small. This yields

$$\begin{aligned} \omega^2 &= (1+2\eta)v_n^2 k_r^2 + \alpha^2 k_z^2 - 2q_1 \frac{2\eta f v_n^2 k_r^2 k_z^2}{k^2 \left(1 - \frac{\beta^2}{\alpha^2} + \frac{2\epsilon k_r^2}{k^2} - \frac{4 f q_2 G}{k^2}\right)} \\ &\approx (1+2\eta)v_n^2 k_r^2 + \alpha^2 k_z^2 - 2q_1 \frac{2\eta f v_n^2 k_r^2 k_z^2}{k^2} \left(1 + \frac{\beta^2}{\alpha^2} - \frac{2\epsilon k_r^2}{k^2} - \frac{4 q_2 f G}{k^2}\right) \,. \end{aligned} \tag{32}$$

The corresponding approximation of G reads

$$\begin{aligned} G &= \frac{2(\epsilon-\delta)k_r^2k_z^2}{fk^2+2\epsilon k_r^2} = \frac{2(\epsilon-\delta)k_r^2k_z^2}{k^2\left(1-\frac{\beta^2}{\alpha^2}+\frac{2\epsilon k_r^2}{k^2}\right)} \\ &\approx \frac{2(\epsilon-\delta)k_r^2k_z^2}{k^2}\left(1+\frac{\beta^2}{\alpha^2}-\frac{2\epsilon k_r^2}{k^2}\right) . \end{aligned} \tag{33}$$

Substitution of equation (30) in equation (29) yields, up to third order in $1/k^2$,

$$\omega^2 \approx (1+2\eta)v_n^2k_r^2+\alpha^2k_z^2-2q_1\frac{2\eta v_n^2k_r^2k_z^2}{k^2}\left[1-\frac{\beta^4}{\alpha^4}-\frac{2\epsilon f k_r^2}{k^2}-\frac{8q_2f(\epsilon-\delta)k_r^2k_z^2}{k^4}\left(1-\frac{\beta^4}{\alpha^4}\right)\right] , \tag{34}$$

or, also neglecting β^4/α^4 in consistency with the above approximations,

$$\omega^2 \approx (1+2\eta)v_n^2k_r^2+\alpha^2k_z^2-2q_1\frac{2\eta v_n^2k_r^2k_z^2}{k^2}\left[1-\frac{2\epsilon f k_r^2}{k^2}-\frac{8q_2f(\epsilon-\delta)k_r^2k_z^2}{k^4}\right] . \tag{35}$$

In effect, equations (31) and (35) can be represented as

$$\omega^2 \approx (1+2\eta)v_n^2k_r^2+\alpha^2k_z^2-2q_1\frac{2\eta v_n^2k_r^2k_z^2}{g\,k^2}\left[g-\frac{2\epsilon k_r^2}{k^2}-\frac{8q_2(\epsilon-\delta)k_r^2k_z^2}{k^4}\right] . \tag{36}$$

with three possible choices for g, being

$$g=f \qquad \text{or} \qquad g=\frac{1}{f} \qquad \text{or} \qquad g=1 . \tag{37}$$

The latter choice of $g=1$ is obtained from setting $\beta=0$. In other words, it is the pseudo-acoustic version of this equation. It reduces the number of parameters describing the wave propagation to the same number used in the previous approximations.

Equation (36) can be conveniently implemented in the mixed space-wavenumber domain by calculating the involved derivatives in the wavenumber domain and then applying space-variable scaling in the space domain. Since the derivative calculations can be carried out with respect to local coordinates for each point in the model space, equation (36) can be immediately used for an implementation in tilted transversely isotropic media in a similar way to the ones indicated by Zhan et al. (2013) or Zhou et al. (2015).

For comparison, we have implemented a low-rank solution (Fomel et al., 2013) to the dispersion relation of the original qP-wave eikonal equation (6). We computed the low-rank approximation matrix using the algebraic reconstruction technique (ART) according to Kaczmarz (1993). The low-rank approximation allows to approximate an arbitrary dispersion relation with any desired precision. It requires a prediction of the rank of the approximation matrix. In the examples in this work, we used always the smallest number that kept the residual below a specified level. Note that the required rank depends on the medium heterogeneity and anisotropy.

NUMERICAL EXAMPLES

To better understand the S-wave modes in the pseudo-acoustic approximation and to demonstrate the quality of the approximations obtained from the above analysis, Schleicher and Costa (2014) have calculated a number of slowness surfaces and modeled wave propagation for a set of differently anisotropic media. Here, we demonstrate the quality of the separable approximations.

Separable approximations

We evaluate the quality of the separable approximations by means of a set of numerical experiments. Figure 1 shows the approximation achieved by equation (31) as compared to the linear approximation of equation (25). While the linear approximation achieves acceptable quality for moderate anisotropy, the strong-anisotropy approximation attains visible improvements for the largest-anisotropy media in Figure 1e

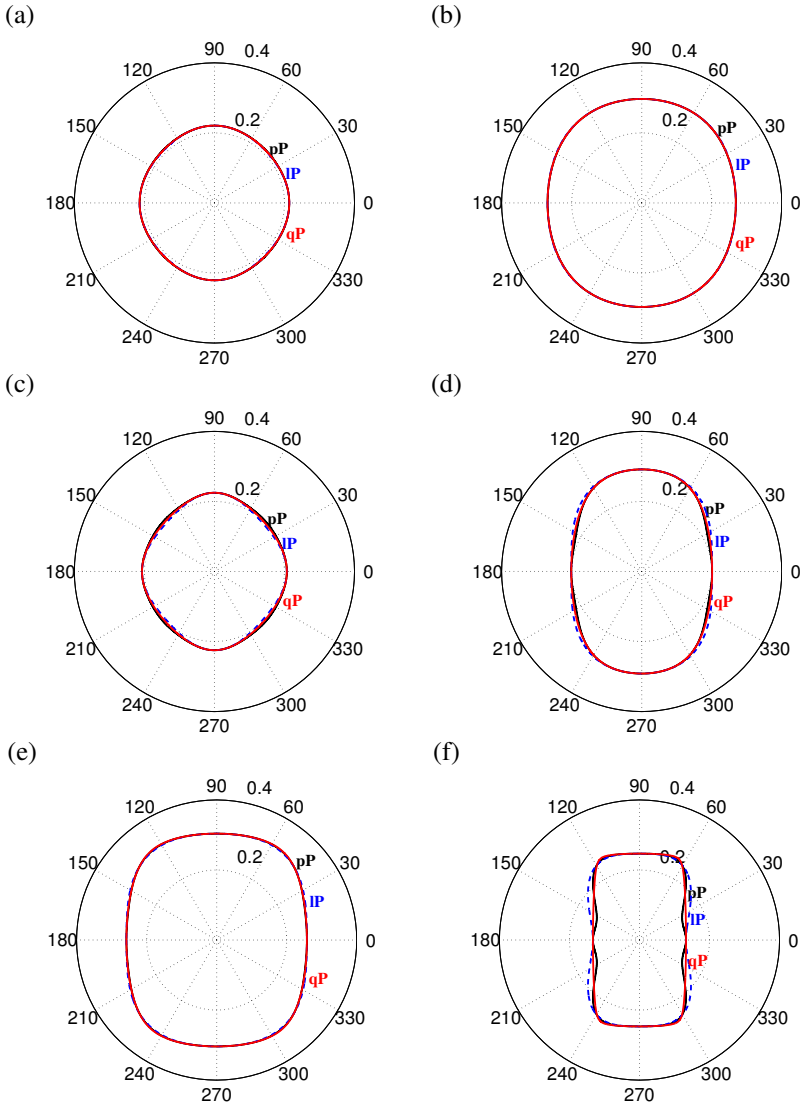

Figure 1: True qP slowness surface (red line) and its separable non-acoustic Padé approximation (dashed blue line) for (a) Mesaverde Mudshale; (b) Taylor Sandstone; (c) Mesaverde Laminated Siltstone; (d) Shale TH-51/13 (e) dry Green River Shale; (f) Biotite Crystal.

and f. Note that for this approximation, there was no apparent advantage in using the anisotropy-dependent Padé coefficients of Schleicher and Costa (2014) over the conventional choice of $q_1 = 1/2$ and $q_2 = 1/4$.

Figure 2 shows the relative error of the slowness in the non-acoustic separable approximations as a function of the propagation angle for the chosen materials. We see that the strong-anisotropy approximation reduces the error by about least 50% even for the materials with smaller anisotropy. The largest reduction is achieved for Taylor Sandstone (Figure 2b), while the least reduction occurs for Mesaverde Laminated Siltstone (Figure 2c).

Figure 2 also shows the relative error of the slowness in the pseudo-acoustic versions ($f = 1$ in equation (31)) of the separable approximations as a function of the propagation angle for the chosen materials. We see that the strong-anisotropy approximation has about the same quality as before, indicating that there is no need for the use of the S-wave velocity as an additional parameter.

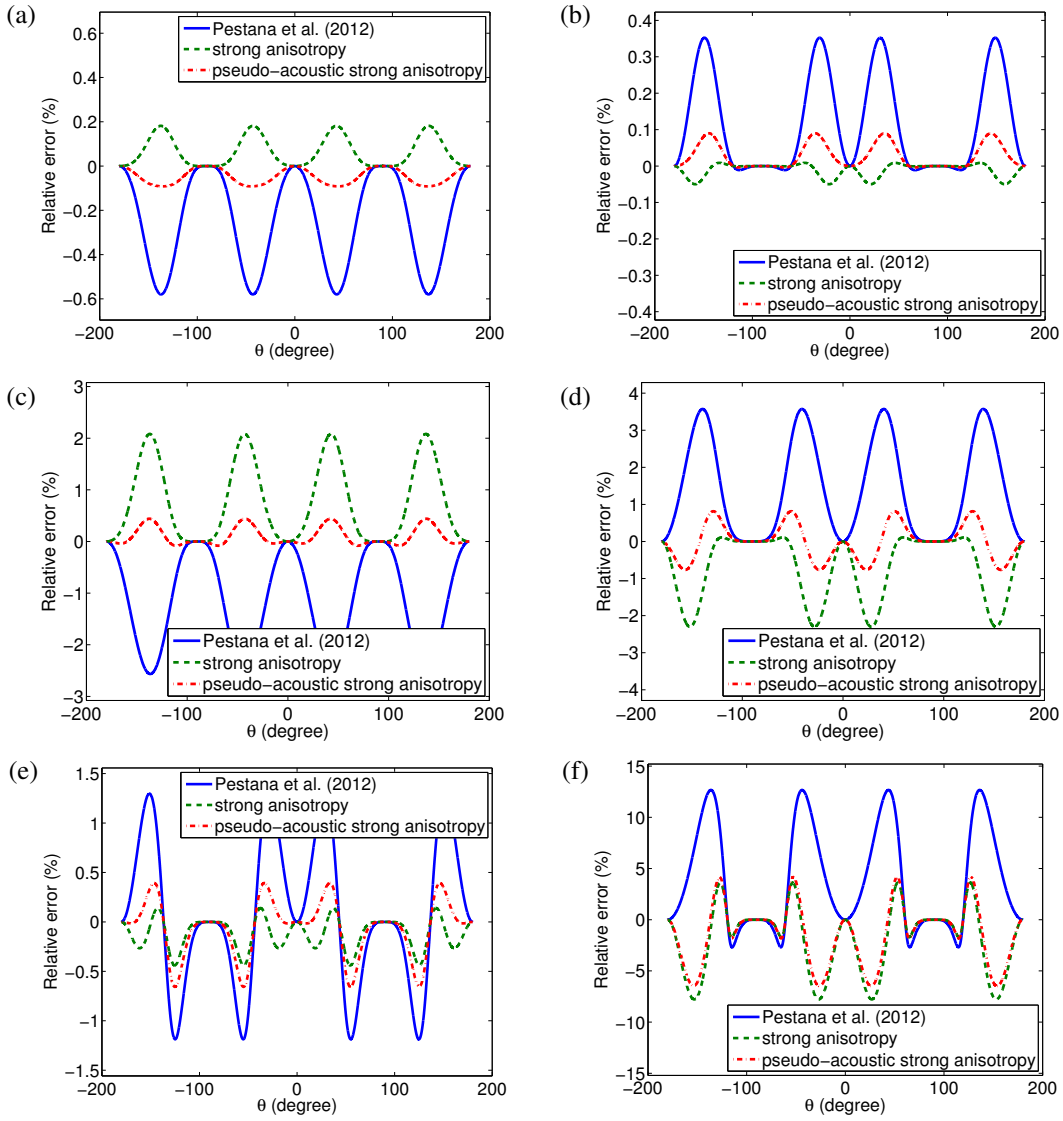

Figure 2: Error of pseudo-acoustic slowness surface for linear (solid blue line) and separable full (dashed green line) and pseudo-acoustic (dash-dotted red line) strong-velocity approximations for (a) Mesaverde Mudshale; (b) Taylor Sandstone; (c) Mesaverde Laminated Siltstone; (d) Shale TH-51/13 (e) dry Green River Shale; (f) Biotite Crystal.

Propagation snapshots

Encouraged by these very good approximations of the slowness surface, we implemented schemes to simulate numerical wave propagation by means of these equations. The numerical tests evaluate the separable approximations (25) and (31), which we implemented in the mixed space-wavenumber domain, and compare them to a low-rank approximation of the original equation (6).

Heterogeneous anisotropy parameters, constant tilt For the first test of the separable approximations, we used an inhomogeneous model, in which both the velocity and the anisotropy parameters are heterogeneous (see parameters in Figure 3). Figure 4 compares the modeling results with the linear separable approximation (a) to the ones with the strong-anisotropy separable approximation (b) and the low-rank approximation (c).

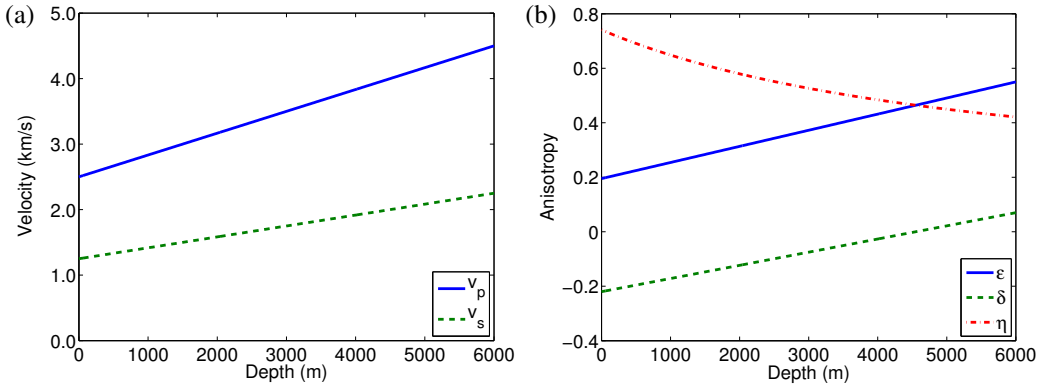

Figure 3: Model parameters of heterogeneous TTI model with constant tilt axis of 30°. (a) Vertical velocities. (b) Anisotropy parameters.

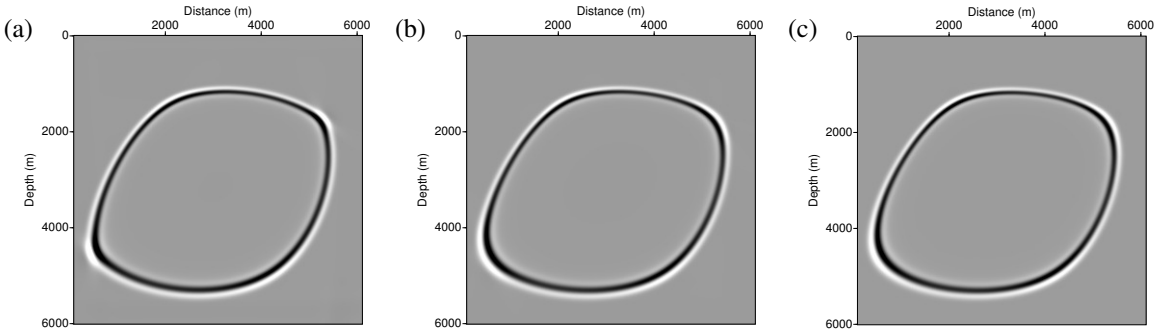

Figure 4: Snapshots of qP wave in a heterogeneous TTI model with constant tilt of 30°. (a) Linear separable approximation. (b) Strong-anisotropy separable approximation. (c) Low-rank approximation.

Heterogeneous anisotropy parameters, varying tilt Our next test used the same model parameters as the previous one, with the TI symmetry axis now varying from 0° to 60°. Figure 5 shows the varying tilt and compares the modeling results with the linear separable approximation (a) to the ones with the strong-anisotropy separable approximation using $g = f$ (b), $g = 1/f$ (c), and $g = 1$ (d), and the low-rank approximation of the square-root equation (e). We see that the second-order approximations resemble the low-rank result more closely than the first-order approximation. Between the second-order approximations, the differences are rather subtle. Closer inspection reveals that the pseudo-acoustic version ($g = 1$) comes closest.

BP TTI Model Our final test consisted of wave simulations in the BP TTI Model (Figure 6). We simulated two shots at the surface at positions $x_s = 32.0$ km and $x_s = 48.0$ km and restricted the model to the solid and dashed boxes, respectively, indicated in Figure 6. We chose these regions for their large variations in anisotropy parameters and tilt angle. For the second shot, we selected the region with the strongest anisotropy and most extreme tilt angles in the model. To test the approximations for even stronger anisotropy, we then repeated the second shot in a model where we multiplied the ϵ values by a factor of two. This leads to about three times larger anellipticity.

Figures 7 to 9 compare snapshots of the modeled wavefields with the separable strong-anisotropy approximation to the corresponding low-rank results. We simulated the first shot at $x_s = 32.0$ km in the area indicated by the solid box in Figure 6. We observe almost perfect coincidence between the two snap shots (Figure 7). For the second shot, simulated in the area indicated by the dashed box in Figure 6, we observe a few subtle differences between the two snapshots (Figure 8). Numerical dispersion of the separable approximation is a little stronger than in the low-rank solution, resulting in slightly broadened wavelets. The main differences, however, lie in the amplitude behaviour. The low-rank solution suffers from stronger amplitude decay in the deeper part of the model than the separable approximation, indicating

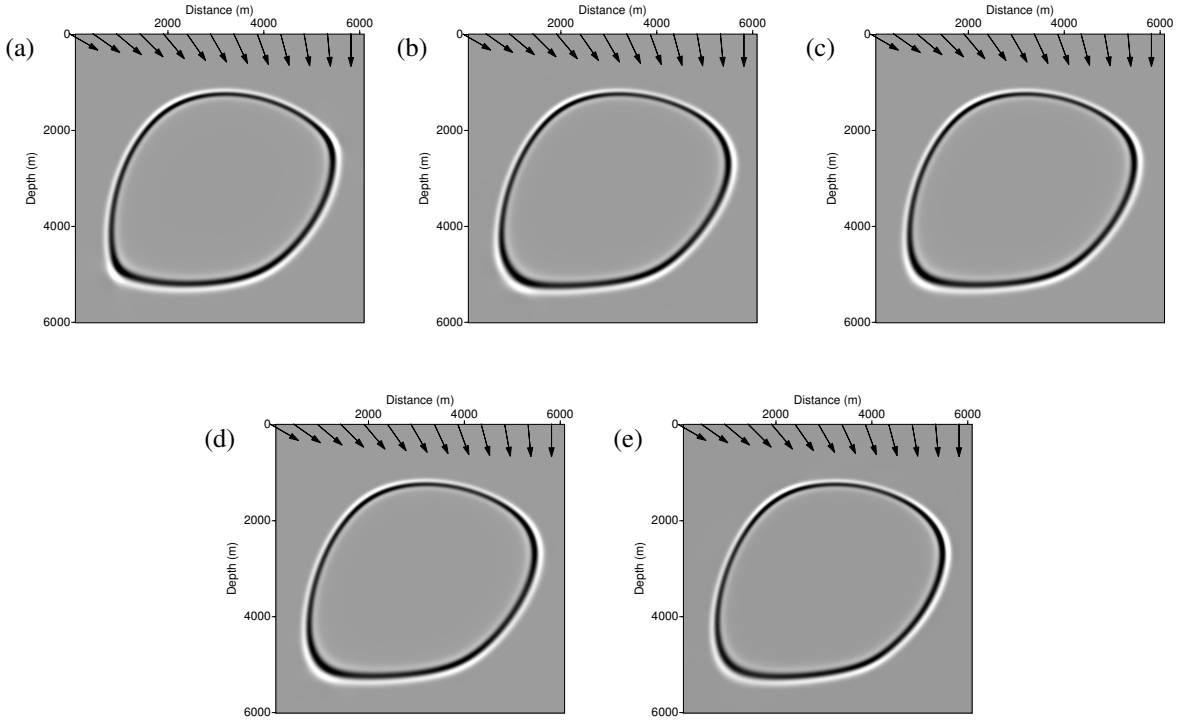

Figure 5: Snapshots of qP wave in a heterogeneous TTI model with variable tilt. Comparison of separable to low-rank approximation. (a) Linear (b) Strong-anisotropy, $g = 1/f$. (c) Strong-anisotropy, $g = f$. (d) Strong-anisotropy, $g = 1$. (e) Low-rank approximation.

that the treatment of geometrical spreading is different. Moreover, some of the reflections have visibly different amplitudes, probably caused by a different treatment of reflection and transmission coefficients. The same kind of differences, though a little more pronounced, are present appear in Figure 9, which compares the corresponding snapshots for the second shot position in the dashed box for the model with doubled ϵ. Regarding the amplitude differences, it should be kept in mind that these approximations of pure qP-wave propagation are meant to reproduce only the kinematic behaviour and cannot be expected to predict correct elastic amplitudes.

CONCLUSIONS

In a continuation of last year's report (Schleicher and Costa, 2014), we have studied approximations to the qP wave dispersion relation. The full pseudo-acoustic qP dispersion relation of Alkhalifah (2000) is actually a coupled equation that describes both qP and a qSV waves. The equation can be uncoupled if the individual eikonal equations are considered. Since these equations contain square roots, they cannot be directly converted into differential approximations. Even their implementation by means of a low-rank approximation might be impaired in heterogeneous and strongly anisotropic media, as indicated by Wu and Alkhalifah (2014). Therefore, Schleicher and Costa (2014) discussed several possible approximations of the square root and compared their quality.

In this report, we start at the Padé approximation to derive a separable approximation that allows for pseudo-spectral implementation in the mixed space-wavenumber domain. This allows to explore its potential to provide an approximation that factors heterogeneity and anisotropy even in strongly anisotropic media in the fashion used by Liu et al. (2009) and Pestana et al. (2012) for weak anisotropy. Our numerical experiments demonstrate that this separable approximation remains valid up to very strong anisotropy. Even for extremely anisotropic Biotite Crystal with $\eta = 7.1875$, the slowness surface was approximated with an error of less than 5%.

Numerical modeling in the more realistic BP TTI model showed that for moderate anisotropy, the results

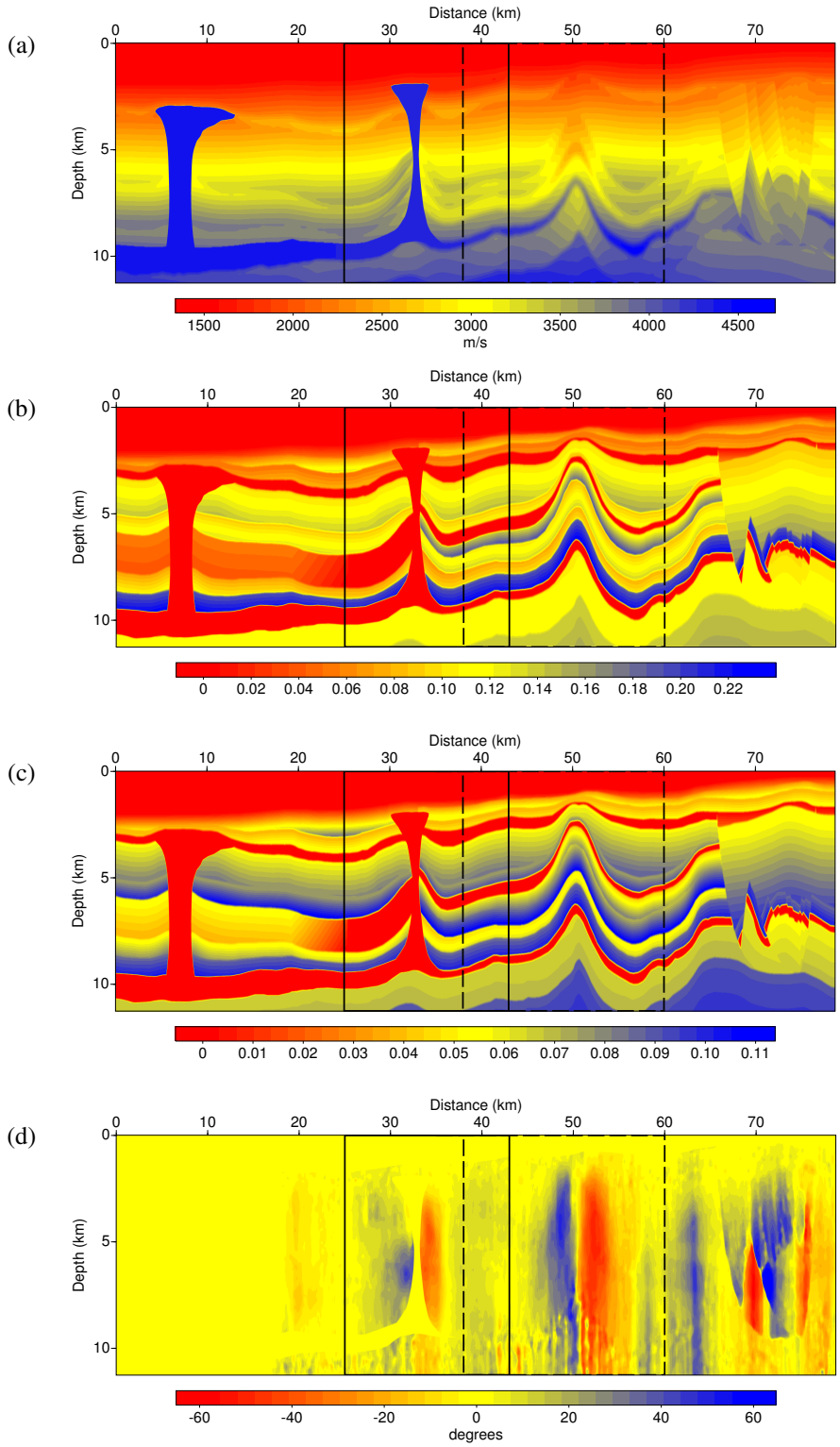

Figure 6: Model parameters of BP TTI model: (a) α; (b) ϵ; (c) δ; (d) tilt angle. Indicated as solid and dashed boxes are the regions used for the two numerical simulations.

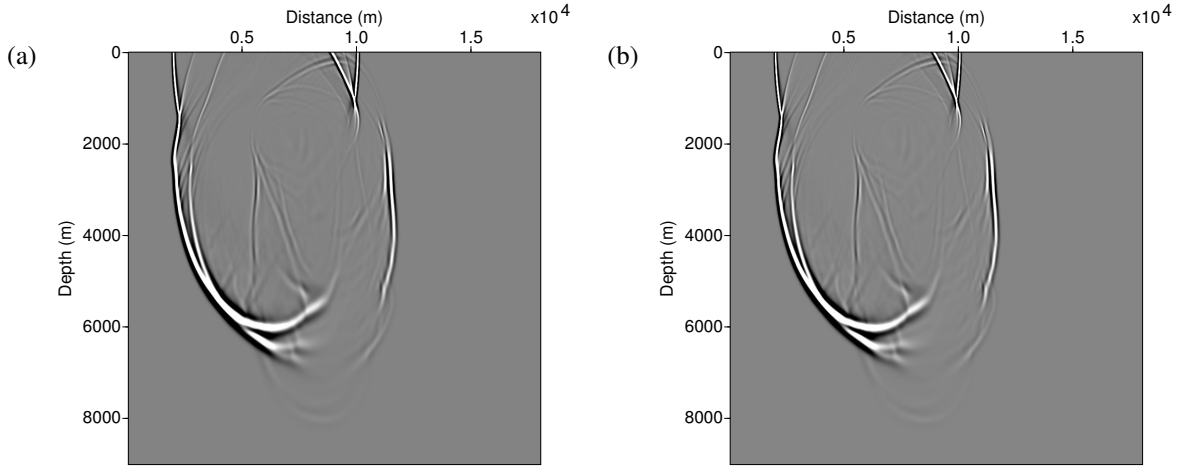

Figure 7: Snapshots of qP wave in the BP TTI model (solid-box region in Figure 6). (a) Strong-anisotropy separable approximation. (b) Low-rank approximation.

of the new separable approximation are virtually identical to those of a low-rank solution. Increasing the anisotropy in this model, we mainly observed differences between the amplitudes. In this respect, it is important to remember that these approximations are derived to mimic the kinematic behaviour of qP waves without regard to amplitudes.

ACKNOWLEDGMENTS

This work was kindly supported by the Brazilian government agencies CAPES, FINEP, and CNPq as well as Petrobras and the sponsors of the *Wave Inversion Technology (WIT) Consortium*.

REFERENCES

Alkhalifah, T. (1998). Acoustic approximations for processing in transversely isotropic media. *Geophysics*, 63(2):623–631.

Alkhalifah, T. (2000). An acoustic wave equation for anisotropic media. *Geophysics*, 65(4):1239–1250.

Alkhalifah, T. (2003). An acoustic wave equation for orthorhombic anisotropy. *Geophysics*, 68(4):1169–1172.

Bloot, R., Schleicher, J., and Santos, L. T. (March, 2013). On the elastic wave equation in weakly anisotropic VTI media. *Geophysical Journal International*, 192(3):1144–1155.

Červený, V. (1985). The application of ray tracing to the numerical modeling of seismic wavefields in complex structures, part A: Theory. In Dohr, G., editor, *Seismic Shear Waves*, volume 15 of *Handbook of Geophysical Exploration, Section I: Seismic*, pages 1–124. Geophysical Press, London – Amsterdam.

Červený, V. (2001). *Seismic Ray Theory*. Cambridge University Press.

Du, X., Fletcher, R., and Fowler, P. J. (2008). A new pseudo-acoustic wave equation for VTI media. In *70th EAGE Annual Conf. and Exhibition Extended Abstract*, page H033. EAGE.

Du, X., Fowler, P., and Fletcher, R. (2014). Recursive integral time-extrapolation methods for waves: A comparative review. *Geophysics*, 79(1):T9–T26.

Fletcher, R., Du, X., and Fowler, P. (2009). Reverse time migration in tilted transversely isotropic (TTI) media. *Geophysics*, 74(6):WCA179–WCA187.

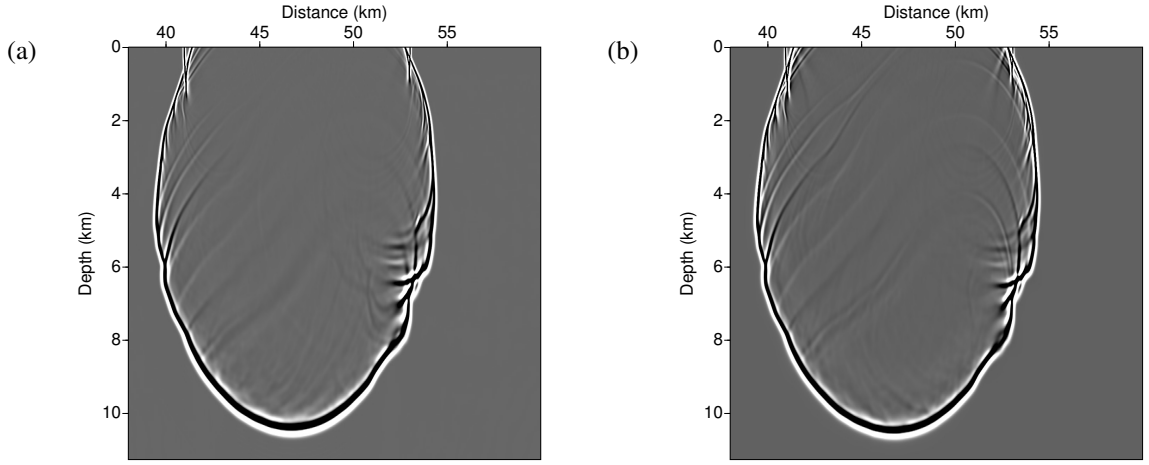

Figure 8: Snapshots of qP wave in the BP TTI model (dashed-box region in Figure 6). (a) Strong-anisotropy separable approximation. (b) Low-rank approximation.

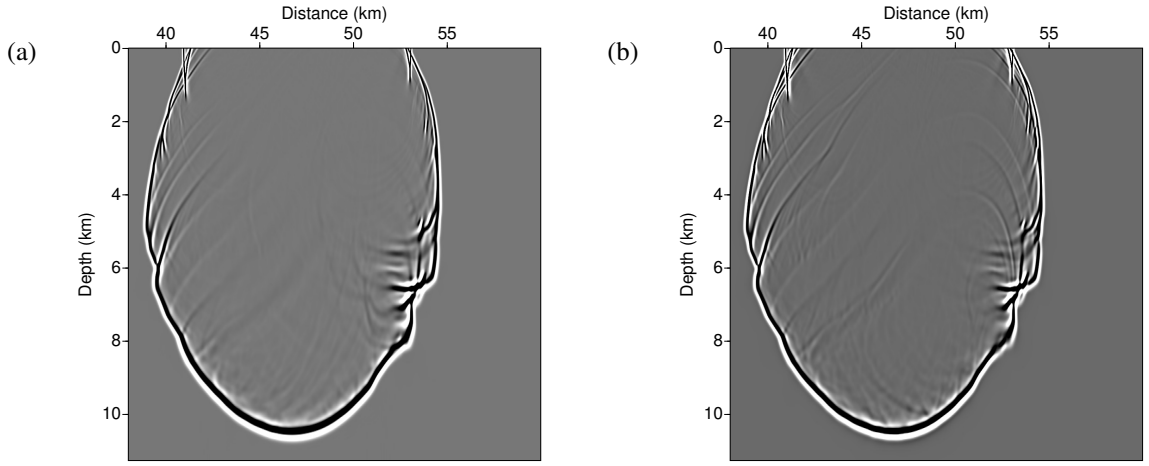

Figure 9: Snapshots of qP wave in the BP TTI model with doubled ϵ (dashed-box region in Figure 6). (a) Strong-anisotropy separable approximation. (b) Low-rank approximation.

Fomel, S., Ying, L., and Song, X. (2013). Seismic wave extrapolation using lowrank symbol approximation. *Geophysical Prospecting*, 61:526–536.

Fowler, P., Du, X., and Fletcher, R. (2010). Coupled equations for reverse time migration in transversely isotropic media. *Geophysics*, 75(1):S11–S22.

Grechka, V., Zhang, L., and Rector, J. (2004). Shear waves in acoustic anisotropic media. *Geophysics*, 69(2):576–582.

Kaczmarz, S. (1993). Approximate solution of systems of linear equations. *International Journal of Control*, 57(6):1269–1271.

Klíe, H. and Toro, W. (2001). A new acoustic wave equation for modeling in anisotropic media. In *SEG Technical Program Expanded Abstracts 2001*, pages 1171–1174.

Le, H. and Levin, S. A. (2014). Removing shear artifacts in acoustic wave propagation in orthorhombic media. In *SEG Technical Program Expanded Abstracts 2014*, pages 486–490.

Liu, G., Fomel, S., Jin, L., and Chen, X. (2009). Stacking seismic data using local correlation. *Geophysics*, 74(3):V43–V48.

Pestana, R. C., Ursin, B., and Stoffa, P. L. (2012). Rapid expansion and pseudo spectral implementation for reverse time migration in VTI media. *J. Geophys. Eng.*, 9:291–301.

Schleicher, J. and Costa, J. C. (2014). Pure qP-wave propagation in VTI media. *Annual WIT report*, 18:258–271.

Song, X. and Alkhalifah, T. (2013). Modeling of pseudoacoustic P-waves in orthorhombic media with a low-rank approximation. *Geophysics*, 78(4):C33–C40.

Sun, J., Fomel, S., and Ying, L. (2016). Low-rank one-step wave extrapolation for reverse time migration. *Geophysics*, 81(1):S39–S54.

Thomsen, L. (1986). Weak elastic anisotropy. *Geophysics*, 51:1954–1966.

Wu, Z. and Alkhalifah, T. (2014). The optimized expansion based low-rank method for wavefield extrapolation. *Geophysics*, 79(2):T51–T60.

Zhan, G., Pestana, R. C., and Stoffa, P. L. (2013). An efficient hybrid pseudospectral/finite-difference scheme for solving the TTI pure p-wave equation. *J. Geophys. Eng.*, 10(2):025004.

Zhou, Y., Wang, H., and Liu, W. (2015). Alternative stable qP wave equations in TTI media with their applications for reverse time migration. *J. Geophys. Eng.*, 12(5):734–744.